

Development of Red-Shifted and Fluorogenic Nucleoside and Oligonucleotide Diarylethene Photoswitches

Theresa Kolmar,^[a] Antonia Becker,^[a] Ronja A. Pfretzschner,^[a] Alina Lelke,^[a] and Andres Jäschke*^[a]

Abstract: The reversible modulation of fluorescence signals by light is of high interest for applications in super-resolution microscopy, especially on the DNA level. In this article we describe the systematic variation of the core structure in nucleoside-based diarylethenes (DAEs), in order to generate intrinsically fluorescent photochromes. The introduction of aromatic bridging units resulted in a bathochromic shift of the visible absorption maximum of the closed-ring form, but caused reduced thermal stability and switching efficiency. The replacement of the thiophene aryl unit by thiazol

improved the thermal stability, whereas the introduction of a benzothiophene unit led to inherent and modulatable turn-off fluorescence. This feature was further optimized by introducing a fluorescent indole nucleobase into the DAE core, resulting in an effective photoswitch with a fluorescence quantum yield of 0.0166 and a fluorescence turn-off factor of 3.2. The site-specific incorporation into an oligonucleotide resulted in fluorescence-switchable DNA with high cyclization quantum yields and switching efficiency, which may facilitate future applications.

Introduction

Light is a powerful and non-invasive trigger that offers the opportunity to modulate biological functions with high spatial and temporal resolution.^[1–7] However, light modulation requires the introduction of a photochromic unit if the biomacromolecule is not light sensitive by itself, which applies to most biomolecules, and especially to DNA. As the efficiency of photomodulation of DNA structure and function will be highest when the photochrome is as close as possible to the oligonucleotide, a synthetic method is desirable that makes a nucleobase part of the photoswitchable unit. Diarylethenes (DAEs) offer high potential for this task and have been applied in various fields, such as materials science^[8–11] or biological chemistry.^[12,13] Classical DAEs evolved from the stilbenes by fixating the double bond into a cyclic system and exchanging the phenyl rings by heteroaryl (most commonly thiophene) units. Finally, the introduction of two methyl groups on the reactive α -carbons of the thiophene rings led to highly fatigue-resistant and thermally stable photoswitches.^[8,9]

Our lab developed a number of 2'-deoxyuridine- and 2'-deoxy-7-deazaadenosine-based DAEs, in which the nucleoside (natural enantiomer) replaced one of the thiophene rings of dithienylethenes, and demonstrated their use in enzymatic reactions as well as in nanotechnology applications (Figure 1A).^[14–17] The comprehensive variation of the substituents at the thiophene moiety led to the identification of 3 high-performance photoswitches with near-quantitative back-and-forth switching and high photo- and thermal stability.^[18,19] These properties were maintained in the environment of an oligonucleotide, and thus allowed the reversible modulation of enzymatic RNA synthesis by light.^[19] However, our optimization failed to achieve the desired strong red-shift of the visible absorbance maximum of the closed-ring form (CF). No matter

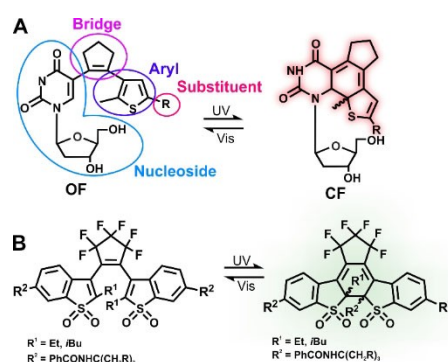


Figure 1. A) Isomerization reaction of dU-based DAEs.^[18] The different parts of the DAEs are marked. All nucleosides shown in this manuscript are the 2'-deoxy-D-ribofuranose derivatives. This graphical presentation was chosen in order to correspond to the nomenclature **Nucleoside**^{Bridge_Aryl_Substituent}. The red shadow of the core structure indicates the colour of the CF in solution. B) Isomerization reaction of a turn-on mode fluorescent DAE.^[21] The green glowing indicates the green fluorescence of the CF.

[a] T. Kolmar, A. Becker, R. A. Pfretzschner, A. Lelke, Prof. Dr. A. Jäschke
 Institute of Pharmacy and Molecular Biotechnology
 Ruprecht-Karls-Universität-Heidelberg
 Im Neuenheimer Feld 364
 69120, Heidelberg (Germany)
 E-mail: jaeschke@uni-hd.de

Supporting information for this article is available on the WWW under <https://doi.org/10.1002/chem.202103133>

© 2021 The Authors. Chemistry - A European Journal published by Wiley-VCH GmbH. This is an open access article under the terms of the Creative Commons Attribution Non-Commercial License, which permits use, distribution and reproduction in any medium, provided the original work is properly cited and is not used for commercial purposes.

which thiophene substituent we chose, $\lambda_{\max, \text{vis}}$ turned out to be limited to 505–510 nm,^[18,19] which will likely limit future applications in biological tissues. Another interesting property known from certain classical DAEs is intrinsic, switchable fluorescence. Most of those photoswitches possess a fluorescent open-ring form (OF), the fluorescence of which is quenched by closing the DAE (turn-off mode).^[20] Recently, a class of DAEs was reported that bear oxidized benzothiophenes as aryl units, which induce a turn-on mode fluorescence with a strongly fluorescent CF isomer (Figure 1B).^[21] These DAEs were applied in super-resolution imaging (RESOLFT) where two distinguishable states (fluorescence on or off) are used to overcome the diffraction limit of light.^[12,22] However, this approach was so far only applied to proteins whereas for nucleic acids imaging such DAE based systems do not yet exist. Super-resolution imaging of nucleic acids has been performed with intercalating fluorescence dyes, but the application in living cells was difficult due to reductive conditions needed to induce a metastable dark state.^[23,24] Other approaches are based on the tagging with fluorogenic aptamer-dye combinations,^[25] which may alter interaction, localization or stability in vivo, or fluorescent in situ hybridisation (FISH),^[26–28] which faces delivery challenges in live cells

In this article we therefore aimed at modifying our established dU-photoswitch architecture in a way that we can achieve a large bathochromic shift of $\lambda_{\max, \text{vis}}$ and also introduce switchable intrinsic fluorescence for future applications in super-resolution microscopy.

Results and Discussion

Exchange of the bridging unit

In order to investigate the influence of the bridging unit, 3 different building blocks (benzothiophene (BT), benzofuran (BF) and methylthiophene (MT)) were selected to replace the cyclopentene. Towards this end, a general synthesis route was established involving a sequence of Suzuki-couplings. The route starts from thiophene boronic acid **1**, which was reacted in a Suzuki coupling to yield the intermediate **2^R**. In the next step another Suzuki reaction with the bridging unit followed, to generate **3X^R** and **4**, which were then lithiated, borylated and coupled to 5-iodo-deoxyuridine to yield the final photoswitches **dU^{BT-TP-R}**, **dU^{BF-TP-R}**, **dU^{MT-TP-Ph}**. (Figure 2A, for nomenclature definition see Table 1). As thiophene (TP) substituents **R**, 4 different moieties ranging from weakly electron-donating (Np) over electron neutral (Ph) to slightly electron-withdrawing (2Py, 4Py) were chosen. These substituents had been shown to improve the fatigue resistance, thermal stability and the composition of the PSS^{UV} for cyclopentene-bridged dU-based DAEs.^[18] BT, BF and MT were introduced with the aim to shift the absorbance in the visible wavelength range in a bathochromic manner, as the conjugated π -system of the CF gets extended by the introduction of these bridging units. To our delight, all new DAEs showed photochromism (Figure 2B, Figure S1), and $\lambda_{\max, \text{vis}}$ of the CF was bathochromically shifted up to

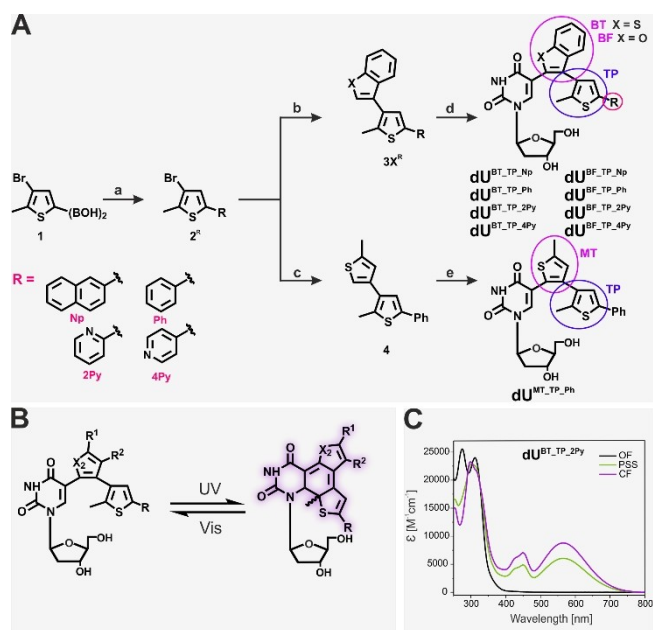


Figure 2. A) Introduction of different bridging moieties: a) R(BOH)₂, Pd(dppf)-Cl₂, Na₂CO₃, THF, 75 °C. b) benzo[b]thiophen-3-ylboronic acid/benzofuran-3-ylboronic acid, Pd(PPh₃)₄, DME/H₂O, 75 °C. c) 1. *n*-BuLi, B(OBu)₃, THF, 2. 4-bromo-2-methylthiophene, Pd(PPh₃)₄, Na₂CO₃, DME/H₂O, 75 °C. d) e) 1. *n*-BuLi, B(OBu)₃, THF, 2. dUI, Pd(dppf)Cl₂, Na₂CO₃, THF/H₂O, 75 °C. The different parts of the DAE are marked. B) Isomerization reaction of the modified photoswitches. C) Absorption spectrum of **dU^{BT-TP-2Py}**.

110 nm, in comparison with the cyclopentene-bridged parent switches (Table 1). The benzothiophene- and methylthiophene-bridged compounds showed the strongest red-shifts, mostly independent of the substituents, emphasizing the high impact of the bridging unit on the entire chromophoric system (Figure 2C). The heteroatom in the 5-membered ring of the bridging unit is of high importance, which is reflected in the smaller bathochromic shift of $\lambda_{\max, \text{vis}}$ (~540 nm) for the benzofuran bridge. This difference is likely due to the higher aromaticity of the benzothiophene and methylthiophene in comparison to benzofuran, leading to a stronger delocalisation of the π -electrons.^[29,30] For all photoswitches, full conversion to the OF was observed after irradiation with visible light. Further investigation of the photophysical properties revealed a high reversibility of back-and-forth switching (92–99%, defined as the relative amount of CF isomer formed after 10 switching cycles, Table 1, Figure S2).

This result indicates that the cyclization and ring opening reaction proceed without significant side reactions.^[31] The thermal stability is strongly dependent on the substituent on the thiophene ring, where photoswitches with electron-withdrawing moieties (2Py, 4Py) showed the highest thermal half-lives at 25 °C (Table 1, Figure S3). In general, the thermal half-lives are lower than for cyclopentene-bridged deoxyuridine DAEs, which may be due to the difference in enthalpy between OF and CF. During the cyclization reaction, the aromatic stabilization energy of the benzofuran, benzothiophene and methylthiophene bridge is lost and therefore the CF is higher in

Table 1. Photophysical properties of photoswitches with different bridging units. Nomenclature: **Nucleoside**^{Bridge_Aryl_Substituent}

	dU ^{BT_TP_Np}	dU ^{BT_TP_Ph}	dU ^{BT_TP_2Py}	dU ^{BT_TP_4Py}	dU ^{BF_TP_Np}	dU ^{BF_TP_Ph}	dU ^{BF_TP_2Py}	dU ^{BF_TP_4Py}	dU ^{MT_TP_Ph}
$\lambda_{\max, \text{PSS}}^{\text{vis}}$ [nm] ^[a]	563	563	565	560	553	549	544	539	580
ϵ [$10^3 \text{M}^{-1} \text{cm}^{-1}$] ^[b]	10.00	8.38	8.76	8.14	12.51	10.22	12.78	10.30	13.35
reversibility [%] ^[c]	95	97	96	90	95	98	98	97	92
thermal stability [h] ^[d]	4	4.5	13	21	26	7	34	25	26
PSS [%] ^[e]	68	68	69	68	62	48	57	56	54
$\phi_{\text{OC}}^{300\text{nm}}$ [f]	0.42	0.50	0.42	0.43	0.21	0.19	0.28	0.32	0.26
$\phi_{\text{CO}}^{300\text{nm}}$ [g]	0.20	0.24	0.19	0.18	0.28	0.22	0.22	0.28	0.16
$\phi_{\text{CO}}^{\text{vis}}$ [h]	0.16 ^[h]	0.18 ^[h]	0.16 ^[h]	0.17 ^[h]	0.24 ^[i]	0.19 ^[i]	0.22 ^[i]	0.29 ^[i]	0.14 ^[h]
$\phi_{\text{OC}}/\phi_{\text{CO}}^{300\text{nm}}$ [j]	2.10	2.08	2.21	2.39	0.75	0.86	1.27	1.14	1.63

^a Wavelength for the absorption maximum in the visible range. ^b Extinction coefficient of the closed ring form at the absorption maximum in the visible range in water/ethanol (2/1). ^c Reversibility: A(t)/A0 at the absorption maximum in the visible range after 10 cycles. ^d Thermal half-lives of the closed ring form at 25 °C. ^e Photostationary state after irradiation with UV-light. ^f Ring, cyclization quantum yields at 300 nm. ^g Ring opening quantum yields at 300 nm. ^h Ring opening quantum yields at 567 nm. ⁱ Ring opening quantum yields at 528 nm. ^j Ratio of ring closing to ring opening quantum yield at 300 nm.

energy than the OF.^[11] For this reason, the energy at room temperature is sufficient to overcome the activation barrier for the thermal ring opening reaction. Another important aspect for any application is the composition of the photostationary state after UV irradiation, PSS^{UV} (Table 1, Figure S4). Switching yields of up to 69% could be obtained, depending on the bridging unit. The highest values were determined for the benzthiophene bridge whereas for the benzofuran and methylthiophene bridge, values of around 55% were measured. These reduced switching yields (compared to their cyclopentene-bridged counterparts) can be explained by the lack of a spectral separation in the UV range (i.e., a wavelength range where the OF absorbs much stronger than the CF) and furthermore by the ratio of the quantum yields for the cyclization and ring opening reaction upon UV irradiation. Whereas for the benzothiophene series this ratio is around 2, for the benzofuran series it was ~1 or even lower (Table 1). It can be concluded that chemical variation of the bridge is much better suited for tuning $\lambda_{\max, \text{vis}}$ than variation of the substituent at the thiophene unit. In our next approach we investigated the influence of different aryl units with the aim of further optimizing photophysical parameters such as the thermal stability or the PSS^{UV} composition.

Exchange of the aryl unit

The thiophene (TP) aryl moiety was replaced by a thiazol (TZ), benzothiophene (BT) or benzofuran (BF) unit, and especially BT revealed high potential for the introduction of photomodulatable fluorescence. To enhance this fluorescence, the BT moiety (either as aryl moiety or as bridging unit) was oxidized to the corresponding sulfone (BT ox), as benzo[b]thiophene-1,1-dioxide-based DAEs are known to be fluorescent.^[21] The synthetic routes started from commercially available precursors and used

several Suzuki-couplings (Figure 3 A, C). The final oxidation of the BT was done with *m*-CPBA in DCM and yielded the oxidized photoswitches without significant side products. The obtained photoswitches all showed photochromism (Fig 3B, Figure S1) with absorption maxima in the visible range that strongly depended on the combination of the aryl moiety and the bridge. With BF as bridging unit, an increased bathochromic shift of $\lambda_{\max, \text{vis}}$ was observed in the following order: BT ox (450 nm) < BT (497 nm) < TZ (509 nm) < TP (549 nm) (Figure 4). The same trend was also seen for the BT- and the MT-bridged series. This order is in good agreement with classical DAEs as the exchange of a thiophene moiety by a thiazol has been reported to induce a hypsochromic shift of $\lambda_{\max, \text{vis}}$ due to the increase in the HOMO-LUMO gap of the closed ring isomer.^[32] Furthermore, theoretical studies of BT- and BT ox-based DAEs revealed that oxidation of the sulphur atom decreases the energy level of the HOMO and therefore also widens the HOMO-LUMO-gap, which results in a blue-shifted absorption maximum.^[33] The HOMO of a symmetrical BT-based DAE is well-distributed over the whole molecule but the lone electron pairs on the sulphur atom create a node in the electron density to its neighbouring atoms. The HOMO can be stabilized by oxidation, which leads to the elimination of the node and therefore lowers the energy of the HOMO, resulting in a higher HOMO-LUMO gap.^[34] The reversibility of all photoswitches was above 94% after 10 cycles with only one exception (dU^{MT_TZ_Ph} : 84%, Table 2, Figure S2) indicating only minor to no side reactions during the cyclization. The thermal stability for the different aryl units is generally high, especially for BT ox as the aryl unit, a thermal half-life of up to 377 h at 37 °C was measured (Table 2, Figure S3). However, for BT ox as bridge (dU^{BT_ox_BF}), a strong decrease of the thermal stability (8.7 h) was observed. This behaviour is in contrast to the literature, where for symmetrical BT-based DAEs a BT ox-bridge was reported to increase the thermal stability.^[35] The introduction of thiazol as aryl unit

Table 2. Photophysical properties of photoswitches with different aryl units. Nomenclature: **Nucleoside**^{bridge_aryl_substituent}

	dU ^{BF_BT}	dU ^{BF_BT}	dU ^{BF_BT_Ph}	dU ^{BF_BT_Np}	dU ^{BT_ox_BF}	dU ^{BT_BF_ox}	dU ^{BF_BT_ox_Ph}	dU ^{BT_Tz_Ph}	dU ^{BF_Tz_Ph}	dU ^{MT_Tz_Ph}
$\lambda_{\text{max, PSS}}^{\text{vis}}$ [nm] ^[a]	515	485	497	491	484	450	450	542	509	549
ϵ [$10^3 \text{M}^{-1} \text{cm}^{-1}$] ^[b]	8.06	6.94	11.60	14.99	12.46	8.48	16.44	8.74	10.90	10.09
reversibility [%] ^[c]	94	99	99	99	99	99.5	99.9	97	99	84
thermal stability [h] ^[d]	107	37	145	210	8.7	377	377	182	104	92
PSS [%] ^[e]	66	54	53	60	17	68	68	65	47	54
$\phi_{\text{OC}}^{300\text{nm}}$ [f]	0.50	0.28	0.31	0.40	0.09	0.24	0.23	0.50	0.29	0.42
$\phi_{\text{CO}}^{300\text{nm}}$ [g]	0.22	0.27	0.28	0.37	0.54	0.22	0.18	0.22	0.27	0.27
$\phi_{\text{CO}}^{\text{vis}}$ [h]	0.18 ^[h]	0.23 ^[i]	0.21 ^[j]	0.20 ^[j]	0.26 ^[j]	0.21 ^[j]	0.15 ^[j]	0.15 ^[h]	0.23 ^[h]	0.18 ^[k]
$\phi_{\text{OC}}/\phi_{\text{CO}}^{300\text{nm}}$ [l]	2.27	1.04	1.11	1.08	0.17	1.09	1.28	2.27	1.07	1.55

^a Wavelength for the absorption maximum in the visible range. ^b Extinction coefficient of the closed ring form at the absorption maximum in the visible range in water/ethanol (2/1) ^c Reversibility: A(t)/A0 at the absorption maximum in the visible range after 10 cycles. ^d Thermal half-lives of the closed ring form at 37 °C. ^e Photostationary state after irradiation with UV-light. ^f Ring cyclization quantum yields at 300 nm, ^g Ring opening quantum yields at 300 nm. ^h Ring opening quantum yields at 528 nm. ⁱ Ring opening quantum yields at 505 nm. ^j Ring opening quantum yields at 470 nm. ^k Ring opening quantum yields at 567 nm. ^l Ratio of ring closing to ring opening quantum yield at 300 nm.

induced a slight red-shift of λ_{em} of around 22 nm and led to a fluorescence increase for **dU**^{BF_BT_Np_ox} and **dU**^{BF_BT_Ph_ox}. After irradiation to the closed-ring isomer, the fluorescence was reduced up to 1.4 fold, demonstrating the ability to reversibly turn off fluorescence by inducing electronic and steric changes in the molecule. However, the switching efficiency of these DAEs is around 68%, which limits the turn-off factor of the fluorescence to 1.4 fold (Figure 5A, B).

Exchange of the nucleobase

To improve the fluorescence modulation, another approach was investigated in which the nucleobase (uracil) was replaced by the fluorescent nucleobase analogue 4-cyanoindole. It mimics the structure of adenine and is able to hybridize with all nucleobases as a universal hydrophobic base.^[37] We recently reported 2'-deoxy-7-deazaadenosine DAEs with near-quantita-

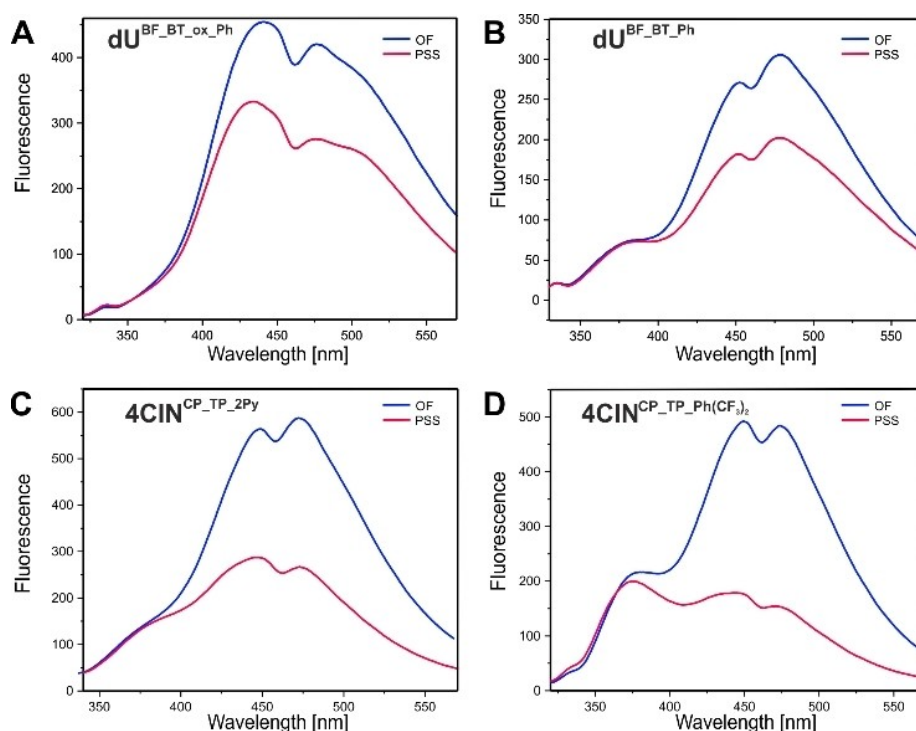


Figure 5. Fluorescence spectra of A) **dU**^{BF_BT_ox_Ph} B) **dU**^{BF_BT_Ph} C) **4CIN**^{CP_TP_2Py} (D) **4CIN**^{CP_TP_Ph(CF₃)₂}. The fluorescence spectrum of the open ring isomer is shown in blue and for the PSS^{UV} in red.

itive switching yields and overall good photophysical properties.^[19] In that study, we used cyclopentene (CP) as bridging unit and introduced a trifluoromethyl-substituted phenyl substituent to the thiophene aryl. This is why we assumed that 4-CN-indole incorporated into a switch with a similar substitution pattern might be a good candidate for achieving high switching yields and at the same time showing efficient turn-off fluorescence. Additionally, we synthesized three other derivatives, including two having the core structure with the best fluorescence properties from the previous section (BF BT Ph). The synthetic route was adapted from our 2'-deoxy-7-deazaadenosine switches and starts from commercially available 4-cyanoindole. First, the introduction of the methyl group at position 1 of 4-cyanoindole was achieved by protecting the nitrogen atom with benzenesulfonyl chloride followed by lithiation and methylation with methyl iodide to obtain **19**. After deprotection of the nitrogen and iodation on the 2-position, a glycosylation with Hoffer's chlorosugar was accomplished to yield **21**. The deprotection of the hydroxyl groups with methanolic sodium hydroxide yielded the final deoxynucleoside analogue **22** (Figure 6A). The final photoswitches were now obtained by a Suzuki coupling with various precursors that combine different bridges, aryl units, and substituents. For the benzofuran-bridged photoswitch with benzothiofene dioxide as aryl moiety (**d4CIN**^{BF_BT_ox_Np}), the oxidation reaction was accomplished with *m*CPBA in DCM at room temperature. The investigation of the photophysical properties revealed a reversible switching behaviour and excellent thermal stabilities for these switches ($\lambda_{\text{max,vis}}$: 530–560 nm, Figure 6B, Figure S1-3). Our presumption regarding the PSS^{UV} composition held true for the

cyclopentene-bridged photoswitches **dCIN**^{CP_TP_2py} and **dCIN**^{CP_TP_Ph(CF)₂}, where switching yields of 86% and 90% could be obtained and at the same time a full conversion to the open form after visible light irradiation was observed. For **dCIN**^{BF_BT_Np} and **dCIN**^{BF_BT_Np_ox}, the PSS^{UV} contained 67% and 48% CF, respectively, highlighting the strong influence of the benzothiofene bridge on the switching efficiency (Figure 6B, Figure S4). The poor spectral separation limits the PSS^{UV} for these two compounds (see Figure S1).

For **dCIN**^{CP_TP_Ph(CF)₂} on the other hand, the ring cyclization quantum yield at 340 nm is high (78%) while the ring opening quantum yield is low (13%). This favourable ratio, combined with the good spectral separation around 340 nm, endow this photoswitch with near-quantitative switching (90%, Figure 6C). The OF isomers of all 4-CN-indole based switches showed bright blue fluorescence at 450–470 nm when excited at 306 nm, whereas the PSS^{UV} showed a reduced fluorescence (Figure 5C, D). In general, the fluorescence intensity was higher than for the benzothiofene-based deoxyuridine switches (except for **dCIN**^{BF_BT_ox_Np}, Figure S5). **dCIN**^{CP_TP_Ph(CF)₂} showed the best combination of photophysical properties and was chosen for further characterization of its fluorescence properties. After cyclization, its fluorescence decreased by a factor of 3.2, allowing for the reversible tuning of the fluorescence in a non-invasive manner (Figure 5C, D). The fluorescence quantum yield of the open ring isomer was determined relative to umbelliferone, that exhibits blue fluorescence with a quantum yield of 0.62 in water (Figure S6/7). The quantum yield of the open-ring isomer is rather low ($\Phi_{\text{Fl}} = 0.0166$), which is likely due to the competition between fluorescence and cyclization, which is

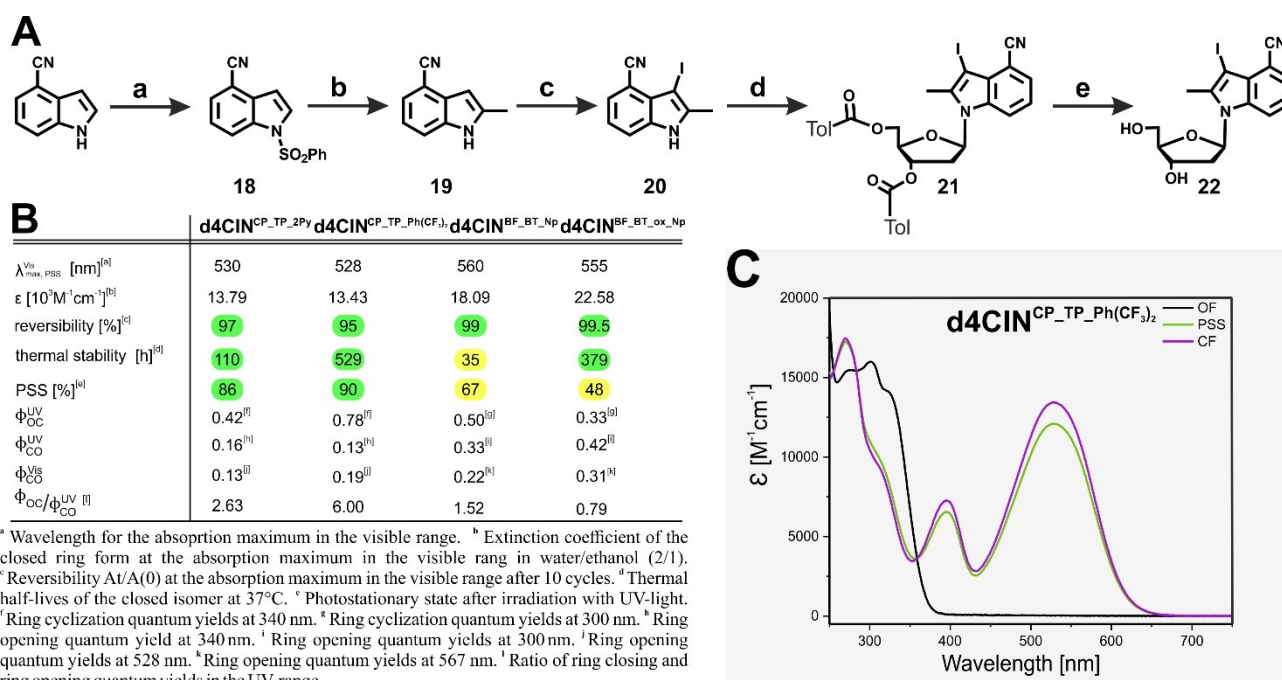


Figure 6. A) Synthesis of **d4CIN**-switches: a) NaH, benzene sulfonyl chloride, THF, RT. b) 1. *n*-BuLi, TMEDA, methyl iodide, THF 2. NaOH, Ethanol, RT. c) I₂, KOH, DMF. d) NaH, Hoffer's chlorosugar, ACN, RT. e) NaOH, methanol. B) Table of photophysical properties. C) Isomer spectra of **d4CIN**-based switch: open form (black), PSS^{UV} (green), calculated closed form (purple).

clearly in favour for cyclization ($\phi_{OC}=0.78$). However, this fluorescence quantum yield is in the same range as those reported for other fluorescent nucleobases.^[38] For an application in biological systems, **dCIN**^{CP-TP-PH(CF₃)₂} seemed to be a promising candidate because of its high switching efficiency (90%) and strong fluorescence modulation.

Fluorescent oligonucleotides

For incorporation into short, non-selfcomplementary oligonucleotides, the deoxynucleoside **dCIN** was protected with dimethoxytritylchloride followed by a Suzuki reaction with the corresponding precursor, yielding the DMT-protected photoswitch **24**. The conversion to the phosphoramidite (**25**) was accomplished in the last step and this building block could be successfully integrated in an oligonucleotide by solid-phase synthesis at various positions (ON-1, ON-2, ON-3, Figure 7A, Figure S8/9). All modified oligonucleotides showed photochromism with slightly bathochromically shifted absorption maxima (Figure 7B/C, Figure S1). For the 4CIN switches, a reduction of the thermal stability was noted that strongly depends on the neighbouring nucleotides (Figure 7C, Fig-

ure S3): Especially for ON-2, where our photoswitch is flanked by two pyrimidines, the thermal stability is decreased dramatically. For ON-1 and ON-3 the flanking bases are one pyrimidine and one purine base, which potentially could inhibit the thermal opening reaction due to steric reasons. In the double strand a different trend of the thermal stability is apparent, indicating a high sensitivity on the surrounding nucleobases. While the nucleoside showed only 5% deterioration after 10 cycles of back-and-forth-switching (Figure 6B), 79–85% of the photochromic oligonucleotides remained intact after the same treatment, indicating a slightly increased deterioration relative to the nucleoside (Figure 7C, Figure S2). In the duplex the deterioration further increased for ON-3, whereas ON-2 and ON-1 showed roughly the same fatigue after 10 cycles compared to the single strand. In the oligonucleotides, the PSS^{UV} was still at an elevated level with switching yields between 78–88% (Figure 7C, Figure S4). The ring cyclization quantum yields decreased only slightly in the single and double strand (compared to the nucleoside), however the ratio of the quantum yields (open vs. closed) is still in favour for the cyclization reaction. We also investigated the thermodynamic stability of the duplexes formed by hybridization with their complementary strands. For ON-1-DS and ON-2-DS, an increase

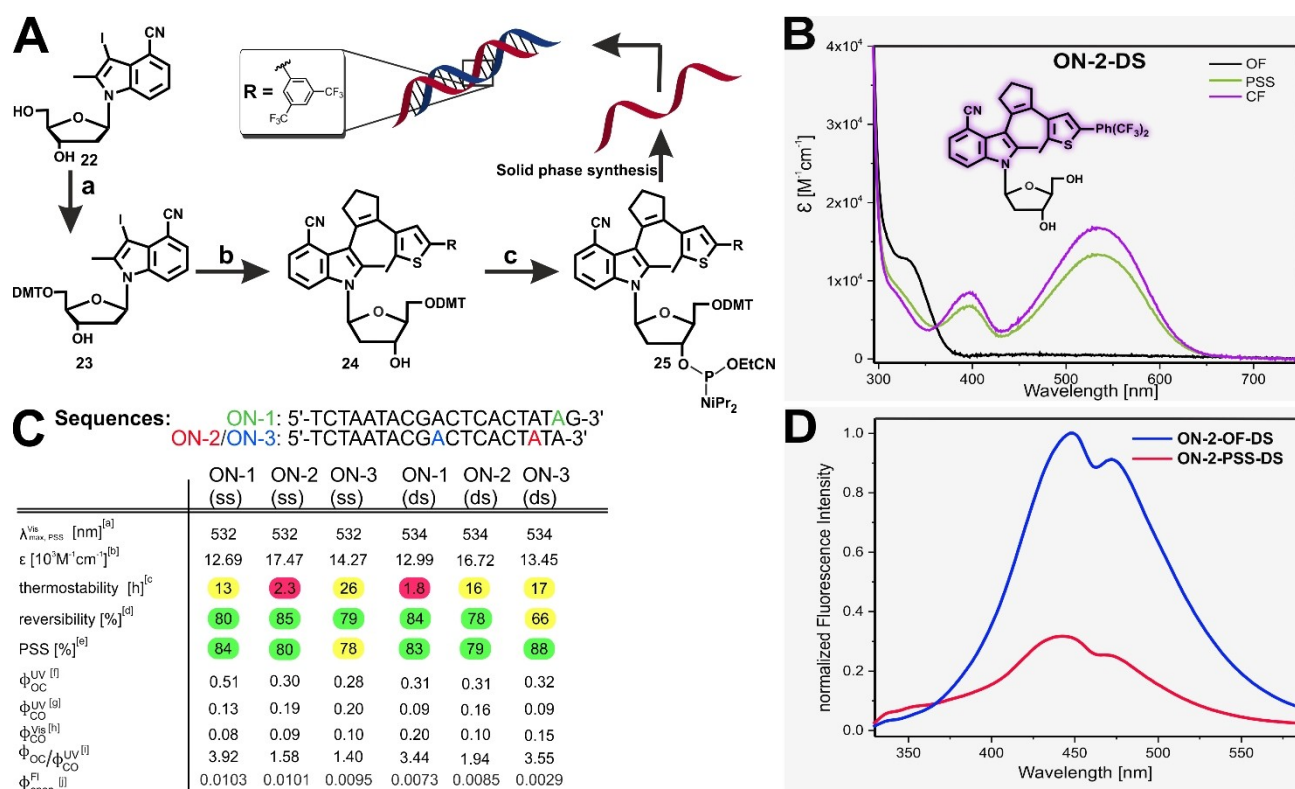


Figure 7. A) Synthesis of a 4CIN-based photoswitch phosphoramidite: a) DMT-Cl, DMAP, pyridine, RT. b) different precursors, Pd(PPh₃)₄, Na₂CO₃, DME/H₂O, 75 °C c) CEP-Cl, NEt₃, DCM, RT. B) Absorbance spectrum of ON-2 in the duplex: Open form (black), PSS (green), calculated closed form (purple). C) Sequences of the modified oligonucleotides. The modified positions are marked in red, blue or green. Table: [a] Wavelength for the absorption maximum in the visible range. [b] Extinction coefficient of the closed-ring form at the absorption maximum in the visible range in TRIS-buffer. [c] Reversibility At/A(0) at the absorption maximum in the visible range after 10 cycles. [d] Thermal half-lives of the closed isomer at 37 °C. [e] Photostationary state (PSS^{UV}) [f] Ring cyclization quantum yields at 340 nm. [g] Ring opening quantum yields at 340 nm. [h] Ring opening quantum yields at 528 nm. [i] Ratio of ring closing and ring opening quantum yields at 340 nm. [j] Fluorescence quantum yields of the open ring isomer ($\lambda_{\text{ex}}=306 \text{ nm}$). D) Fluorescence spectra of ON-2 in the duplex of the open ring isomer (OF) and in the duplex (DS).

of the melting temperatures (T_m) compared to the natural duplex was apparent, indicating a stabilising effect of the modified nucleotide (Figure S10). In contrast, ON-3-DS showed a decrease of 7.5 °C, which leads to the assumption that the photoswitchable nucleotide is forced into the syn-conformation by the neighbouring G, as described recently.^[19] The fluorescence quantum yields decreased by a factor of 1.6 after incorporation into a single DNA strand ($\Phi_{Fl} = 0.00103\text{--}0.0095$). After the formation of the duplex, the decrease of the quantum yields was strongly position-dependent. Whereas for ON-1 and ON-2 only a small decrease was observed, for ON-3 a strong quenching of the fluorescence was apparent (Figure 7C, Figure S5). This quenching could be assigned to the proximity of a guanosine in the complementary strand of ON-3, which is also described in literature.^[39] The turn-off factors upon photo-switching vary depending on the environment of the single strand or duplex. For ON-1, this factor is around 2.4, both in the duplex and in the single strand, whereas for ON-2 and ON-3 this factor increases from SS to DS (2.05→3.03, 2.2→2.76). All in all, ON-2 showed the best performance, when applied in a duplex with a turn-off factor of 3, which is comparable with the free nucleoside (Figure 7D).

Conclusion

This article gives a comprehensive insight in the structural variability of nucleoside-based DAEs, where every part of the photochromic unit was modified. When we first reported nucleoside-based DAEs^[14], we (and also the reviewers) assumed that we had been very lucky and by chance picked a combination of structural components that provided photochromism. The current study demonstrates that the photochromic core structure is very robust, and all its parts can be exchanged without losing photochromism. It was revealed that especially the benzothiophene and methylthiophene bridging units lead to strong bathochromic shifts of $\lambda_{max,vis}$ and in combination with thiazol as aryl unit also improved thermal stabilities were apparent. The introduction of benzothiophene and its oxidized form enabled us to reversibly modulate the fluorescence by switching the photoswitch between its two isomers. Additionally, the fluorescence modulation could be enhanced by the introduction of 4-cyanoindole as nucleobase analogue, which exhibits blue fluorescence in its open form that could be quenched with a turn-off factor of 3.2. Due to its high switching yield and fluorescence modulation, **d4CIN**^{CP,TP-Ph(CF₃)₂} was introduced into an oligonucleotide at different positions. In the environment of an oligonucleotide, fluorescence modulation was retained and found to be slightly dependent on the neighbouring nucleobases. To the best of our knowledge, this is the first time that a fluorescent nucleobase, which is part of a DAE, allows to reversibly modulate its fluorescence. For the use in super-resolution microscopy, further optimizations are needed, to ensure proper quenching of the fluorescence and high quantum yields.

Acknowledgements

The authors thank S. M. Büllmann for discussion of the manuscript. We acknowledge H. Rudy, D. Wolf and T. Timmermann for technical assistance. We also acknowledge H. Derondeau (LMU Munich) for her help in calculating the quantum yields. Open Access funding enabled and organized by Projekt DEAL.

Conflict of Interest

The authors declare no conflicts of interest.

Keywords: diarylethenes · fluorescence modulation · nucleic acids · photochromism · photoresponsive DNA

- [1] C. Brieke, F. Rohrbach, A. Gottschalk, G. Mayer, A. Heckel, *Angew. Chem. Int. Ed.* **2012**, *51*, 8446–8476; *Angew. Chem.* **2012**, *124*, 8572–8604.
- [2] A. Gautier, C. Gauron, M. Volovitch, D. Bensimon, L. Jullien, S. Vriz, *Nat. Chem. Biol.* **2014**, *10*, 533–541.
- [3] A. Jäschke, *FEBS Lett.* **2012**, *586*, 2106–2111.
- [4] W. Szymański, J. M. Beierle, H. A. V. Kistemaker, W. A. Velema, B. L. Feringa, *Chem. Rev.* **2013**, *113*, 6114–6178.
- [5] J. Bath, A. J. Turberfield, *Nat. Nanotechnol.* **2007**, *2*, 275–284.
- [6] V. I. Minkin, in *Molecular Switches* (Eds.: B. L. Feringa, W. R. Browne), Wiley-VCH, Weinheim, **2011**, pp. 37–74.
- [7] S. Ludwig, H. Bayley, in *Dynamic Studies in Biology: Phototriggers, Photoswitches and Caged Biomolecules* (Eds.: M. Goeldner, R. Givens), Wiley-VCH, Weinheim, **2005**, pp. 253–340.
- [8] M. Irie, *Chem. Rev.* **2000**, *100*, 1685–1716.
- [9] M. Irie, T. Lifka, S. Kobatake, N. Kato, *J. Am. Chem. Soc.* **2000**, *122*, 4871–4876.
- [10] M. Irie, T. Lifka, K. Uchida, S. Kobatake, Y. Shindo, *Chem. Commun.* **1999**, 747–748.
- [11] M. Irie, M. Mohri, *J. Org. Chem.* **1988**, *53*, 803–808.
- [12] B. Roubinet, M. Weber, H. Shojaei, M. Bates, M. L. Bossi, V. N. Belov, M. Irie, S. W. Hell, *J. Am. Chem. Soc.* **2017**, *139*, 6611–6620.
- [13] I. V. Komarov, S. Afonin, O. Babii, T. Schober, A. S. Ulrich, *Chem. Eur. J.* **2018**, *24*, 11245–11254.
- [14] M. Singer, A. Jäschke, *J. Am. Chem. Soc.* **2010**, *132*, 8372–8377.
- [15] M. Singer, A. Nierth, A. Jäschke, *Eur. J. Org. Chem.* **2013**, 2766–2769.
- [16] H. Cahová, A. Jäschke, *Angew. Chem. Int. Ed.* **2013**, *52*, 3186–3190; *Angew. Chem.* **2013**, *125*, 3268–3272.
- [17] C. Sarter, M. Heimes, A. Jäschke, *Beilstein J. Org. Chem.* **2016**, *12*, 1103–1110.
- [18] T. Kolmar, S. M. Büllmann, C. Sarter, K. Höfer, A. Jäschke, *Angew. Chem. Int. Ed.* **2021**, *133*, 8164–8173.
- [19] S. M. Büllmann, T. Kolmar, P. Slawetzki, S. Wald, A. Jäschke, *Chem. Commun.* **2021**, *57*, 6596–6599.
- [20] T. Fukaminato, *J. Photochem. Photobiol. C* **2011**, *12*, 177–208.
- [21] K. Uno, M. L. Bossi, M. Irie, V. N. Belov, S. W. Hell, *J. Am. Chem. Soc.* **2019**, *141*, 16471–16478.
- [22] K. Uno, A. Aktalay, M. L. Bossi, M. Irie, V. N. Belov, S. W. Hell, *Proc. Natl. Acad. Sci. USA* **2021**, *118*, 1–6.
- [23] A. G. Godin, B. Lounis, L. Cognet, *Biophys. J.* **2014**, *107*, 1777–1784.
- [24] C. Flors, *Photochem. Photobiol. Sci.* **2010**, *9*, 643–648.
- [25] M. Sunbul, J. Lackner, A. Martin, D. Englert, B. Hacene, F. Grün, K. Nienhaus, G. U. Nienhaus, A. Jäschke, *Nat. Biotechnol.* **2021**, *39*, 686–690.
- [26] A. M. Femino, F. S. Fay, K. Fogarty, R. H. Singer, *Science* **1998**, *280*, 585–590.
- [27] A. Raj, P. Van Den Bogaard, S. A. Rifkin, A. Van Oudenaarden, S. Tyagi, *Nat. Methods* **2008**, *5*, 877–879.
- [28] R. Jungmann, R. B. McCole, B. J. Bellevue, A. N. Boettiger, M. S. Avendan, C. Y. Fonseka, J. Erceg, E. F. Joyce, C. Kim-kiselak, M. A. Hannan, H. G. Hoang, D. Colognori, J. T. Lee, W. M. Shih, *Nat. Commun.* **2015**, 7147.
- [29] M. Szajda, J. N. Lam, in *Compr. Heterocycl. Chem. II A Rev. Lit. 1982–1995* (Eds.: A. R. Katritzky, C. W. Rees, F. V. Scriven), Elsevier, Oxford, **1996**, pp. 471–479.

- [30] G. E. Zhussupova, A. I. Zhussupova, *Procedia - Soc. Behav. Sci.* **2015**, *191*, 1247–1254.
- [31] M. Herder, B. M. Schmidt, L. Grubert, M. Pätzelt, J. Schwarz, S. Hecht, *J. Am. Chem. Soc.* **2015**, *137*, 2738–2747.
- [32] S. Takami, L. Kuroki, M. Irie, *J. Am. Chem. Soc.* **2007**, *129*, 7319–7326.
- [33] T. Ichikawa, M. Morimoto, H. Sotome, S. Ito, H. Miyasaka, M. Irie, *Dyes Pigm.* **2016**, *126*, 186–193.
- [34] Y. C. Jeong, J. P. Han, Y. Kim, E. Kim, S. I. Yang, K. H. Ahn, *Tetrahedron* **2007**, *63*, 3173–3182.
- [35] Y. C. Jeong, D. G. Park, I. S. Lee, S. I. Yang, K. H. Ahn, *J. Mater. Chem.* **2009**, *19*, 97–103.
- [36] S. Takami, S. Kobatake, K. Tsuyoshi, M. Irie, *Chem. Lett.* **2003**, *32*, 892–893.
- [37] K. T. Passow, D. A. Harki, *Org. Lett.* **2018**, *20*, 4310–4313.
- [38] N. J. Greco, R. W. Sinkeldam, Y. Tor, *Org. Lett.* **2009**, *11*, 1115–1118.
- [39] G. T. Hwang, *Molecules* **2018**, *23*, 124.

Manuscript received: August 27, 2021

Accepted manuscript online: September 14, 2021

Version of record online: October 19, 2021